Taylor & Francis
Taylor & Francis Group

Canadian Journal of Remote Sensing
Journal canadien de télédétection

ISSN: 0703-8992 (Print) 1712-7971 (Online) Journal homepage: http://www.tandfonline.com/loi/ujrs20

Monitoring Hydro Temporal Variability in Alberta, Canada with Multi-Temporal Sentinel-1 SAR Data

Evan R. DeLancey, Jahan Kariyeva, Jerome Cranston & Brian Brisco

To cite this article: Evan R. DeLancey, Jahan Kariyeva, Jerome Cranston & Brian Brisco (2018): Monitoring Hydro Temporal Variability in Alberta, Canada with Multi-Temporal Sentinel-1 SAR Data, Canadian Journal of Remote Sensing, DOI: 10.1080/07038992.2018.1417734

To link to this article: https://doi.org/10.1080/07038992.2018.1417734

CANADIAN JOURNAL OF REMOTE SENSING
2018, VOL. 44, NO. 1, 1–10
https://doi.org/10.1080/07038992.2018.1417734

Taylor & Francis
Taylor & Francis Group

Monitoring Hydro Temporal Variability in Alberta, Canada with Multi-Temporal Sentinel-1 SAR Data

Evan R. DeLancey[a], Jahan Kariyeva[a], Jerome Cranston[a], and Brian Brisco[b]

[a]Alberta Biodiversity Monitoring Institute, University of Alberta, Edmonton, AB T6G 2R3, Canada; [b]Canada Centre for Mapping and Earth Observation, Natural Resources Canada, 560 Rochester St., Ottawa, ON K1S 5K2, Canada

ABSTRACT

Freely available high temporal and spatial resolution synthetic aperture radar (SAR) satellite data such as Sentinel-1 have made it possible for almost near-real time monitoring of surface water extent. We present a method to track temporal variability in surface water extent, hereafter hydro temporal variability (HTV) in Alberta, Canada. Multi-temporal Sentinel-1-C band SAR data was used to classify each pixel in a pixel stack across time into water or non-water. This dataset can tell the percent of time a given 10 m × 10 m pixel was seen as open water. HTV was then summarized by calculating the percentage of the total pixel stack, which was detected as water. Comparison to the waterbodies in the Government of Alberta Base Features Hydrography Polygon dataset shows that the HTV dataset is able to differentiate between permanent and recurring lakes as well as capture rivers with a width of over 30 m. It is anticipated that the methodology presented here will be further enhanced and refined with imagery available for 2018 and beyond, due to now operational Sentinel-1B satellite and future RADARSAT Constellation Mission (2018), which will both provide improved data opportunities.

RÉSUMÉ

Les satellites à aperture synthétique à haute résolution temporelle et spatiale, dont *Sentinel-1*, permettent de faire le suivi des étendues d'eau presqu'en temps réel. Nous présentons une méthode, ci-après appelée variabilité temporelle hydrologique (VTH), qui permet de faire le suivi systématique de la variabilité temporelle des étendues d'eau de l'Alberta, Canada. Les données multi-temporelles en provenance de la bande C du satellite *Sentinel-1* ont été utilisées afin de classifier chaque pixel d'une série temporelle de pixels comme étant soit «eau» ou «autre». Cette série de données temporelles permet d'estimer la proportion de temps pendant laquelle un pixel de 10 m est classifié comme étant un pixel d'eau ou autre. Lorsque comparée à la couche de données hydrographique de base (*Base Features Hydrography Polygon*) produite par la Gouvernement de l'Alberta, la méthode VTH permet de classifier les étendues d'eau selon leur hydropériode (e.g., permanent, semi-permanent, saisonnier) en plus de faire le suivi des cours d'eau d'une largeur de plus de 30 m. La méthode présentée pourra éventuellement être raffinée en utilisant de nouvelles données produites par le satellite *Sentinel-1B* qui fut mis en opération en 2016 ou encore par l'éventuelle *RADARSAT Constellation Mission* prévue pour 2018.

ARTICLE HISTORY
Received 5 June 2017
Accepted 13 November 2017

Introduction

About 9% or 891,163 km^2 of Canada is covered by fresh water, which offers a range of environmental and socio-economic benefits and services. With fast paced climate change and increased anthropogenic use of fresh water resources, scientifically sound and robust monitoring of these resources is essential. Alberta provides a diverse set of waterbodies that range from deep mountainous lakes in the west, to ephemeral kettle lakes in the semi-arid prairie pothole regions, to meandering rivers, to peatlands in the northern boreal forest areas. Some of these waterbodies are undergoing rapid and irrevocable change due to anthropogenic pressures, including agriculture, livestock operations, forestry practices, oil and gas development, and population growth (Schindler and Donahue 2006). It is estimated that up to 70% of wetlands in southern Alberta have already been drained or permanently modified (Ducks Unlimited 2017). Additionally, there is evidence that changes in ocean temperatures due to climate change is starting to contribute to mid-latitude drying in North America (Hoerling and Kumar 2003). It appears that anthropogenic and naturally driven climate changes are both leading towards declining fresh water availability in Alberta and the western Prairie Provinces, potentially leading towards a future water crisis (Schindler and Donahue 2006).

With this knowledge, the near-real time monitoring of surface water should be a priority. In-situ lake level and river measurements along with water polygons interpreted from air photos are two methods used to

CONTACT Evan R. DeLancey edelance@ualberta.ca

monitor Alberta waterbodies (Environment and Climate Change Canada 2015; Alberta Environment and Parks, Government of Alberta 2004). In-situ measurements, such as the National Hydrological Service (Environment and Climate Change Canada 2015), are great for tracking waterbody fluctuations but it is nearly impossible to track all of Alberta's waterbodies. Human photo-interpreted waterbody inventories, such as the Government of Alberta Base Features Hydrography Polygons (Alberta Environment and Parks, Government of Alberta 2004) provide great spatial coverage of Alberta's waterbodies but are limited to a certain point in time, which makes tracking lake level fluctuations and recurring waterbodies very difficult. Monitoring waterbodies using satellite imagery with high spatial and temporal resolution (Pultz et al. 1997; Pekel et al. 2016; e.g., Sentinel) provides a promising alternative to these methods as it offers complete spatial coverage and frequent revisits.

Both optical and radar remote sensing methods are well suited for identifying standing water (Töyrä et al. 2001; Brisco 2015) due to the low reflectance of water in the visible to near-infrared (optical) and the specular reflectance of water (radar). The Copernicus mission (European Space Agency 2014) with freely available 10-m resolution radar (Sentinel-1) and optical (Sentinel-2) with 6- and 5-day revisit time, respectively, provides a great option for near-real time monitoring of waterbodies in Alberta. Due to the prevalence of summer cloud cover in Alberta, especially at higher latitudes and altitudes (Wilson and Jetz 2016), optical remote sensing may not be well suited for consistent waterbody monitoring in Alberta. This makes Sentinel-1 C band radar the ideal candidate for tracking fluctuations in Alberta waterbodies' extents on a weekly basis. The Sentinel-1 data with its 6-day revisit time (as of October 2016) proves to be a great source and tool for water monitoring as the radar sensor is capable of detecting standing water (Malenovsky et al. 2012; Brisco 2015) at all times (day and night) and is not limited by cloud cover or haze.

Synthetic aperture radar (SAR) has a long history of use for surface water monitoring, flood mapping, and wetland mapping (Pultz et al. 1997; Töyrä et al. 2001; Townsend 2002; Töyrä and Pietroniro 2005; Brisco et al. 2008, 2009; Bolanos et al. 2016; Twele et al. 2016). In theory, land and water are easy to distinguish with SAR due to the specular reflection of water resulting in low backscatter (Henderson and Lewis 1998; Töyrä et al. 2001; Brisco 2015). Land surfaces in the form of vegetation, bare earth, or human footprint features will generally have a moderate to high backscatter signal due to diffuse, or double bounce reflection (Henderson and Lewis 1998; Töyrä et al. 2001; Brisco 2015). In practice, differentiating land from water can be hard due to wind-induced roughness in waterbodies, and varying incidence angles (Bolanos et al. 2016). Given low wind and consistent incidence angles, image thresholding can be an effective method for surface water identification (Brisco et al. 2009; White et al. 2014). In other cases, thresholding combined with texture information or segmentation algorithms are used to classify standing water (Martinis et al. 2009; Li and Wang 2015). If there are many repeat images for an area the standard deviation (SD) across time, i.e., temporal SD can be useful for identifying water because water will have a higher SD due to waves (unless the water is perfectly calm) while vegetation backscatter should be relatively constant (the exception being agriculture; Santoro and Wugmüller 2014; Santoro et al. 2015).

The key objective for this study is to develop an operational method for calculating the percent of time a 10-m Sentinel-1 pixel is detected as water throughout the 2014–2017 spring and summer months. Now that the two Sentinel-1 satellites are fully operational, this method should be ideal for testing in 2018 spring and summer. This method should result in a dataset where each value will represent the percent of time water was detected in a given 10-m pixel. This dataset, hereafter termed as the hydro temporal variation (HTV) dataset, can hopefully differentiate permanent versus recurring lakes, track seasonal expansion and recession of lake boundaries, and track seasonally flooded areas. Measuring the fluctuation in waterbody level has been done with SAR for smaller areas and or individual lakes (Bartsch et al. 2009; Brisco et al. 2009; Ding and Li 2011; Gstaiger et al. 2012; Yesou et al. 2016) and it has been done globally with Landsat data (Pekel et al. 2016). The proposed HTV product appears to be one of the first ones created to be applicable for large-scale, high resolution, multi-temporal mapping of surface water extent using SAR.

Methods

Data and SAR processing

The HTV dataset was calculated with Sentinel-1 C-band (S1) SAR data (European Space Agency 2014, 2015, 2016). All S1 images were gathered and processed in Google Earth Engine (GEE; Google Earth Engine Team 2015). GEE stores S1 ground range detected scenes, which have been pre-processed with the Sentinel-1 Toolbox (Sentinel Application Platform–Sentinel-1 Toolbox). These pre-processing steps include thermal noise removal, radiometric calibration, and terrain correction (Google Earth Engine Team 2015). S1 images were further processed in the GEE environment by performing an incidence angle correction (Gauthier et al. 1998) and smoothing with a

Table 1. Summary of chosen water and wind speed thresholds for HTV dataset calculation.

Zone	Water threshold (dB)	Wind speed threshold (km/h)	Image date range
grasslands	<−17.5	<9	April, 1st-October 31st
boreal	<−15.1	<9	May 1st-September 30th

3 × 3 Sigma Lee filter (Lee et al. 2009; credit to Guido Lemoine for GEE code).

S1 images intersecting with Alberta during ice-free months were gathered for the time period April 1, 2014–August 5, 2017 (see Table 1 for what defines ice-free months). Winter months were not included as most lakes in Alberta are frozen from October/November to March/April. Additionally, only images with a 10-m resolution were used, which resulted in the exclusion of HH or HV polarizations as these images are only available in 40-m resolution. The VV polarization mode was used for the analysis as it had far more revisits over Alberta when compared to the other polarization modes (VV-VH, HH, HH-HV); however, Brisco (2015) and Bolanos et al. (2016) state that other polarizations are more suitable for water detection but the VV polarization is still very useful (Kasischke and Bourgeau-Chavez 1997). This resulted in a temporal pixel stack of anywhere from 1 to 100 across Alberta.

The processing of the HTV dataset was split into 2 regions (Figure 1). The first region is the grasslands region of southeast Alberta, which is predominately covered by native grasslands or agriculture. The second region is the boreal (boreal forest) region of northern and western Alberta, which is dominated by forests. These regions were delineated using the Alberta natural regions dataset (Alberta Parks 2015). The grassland and parkland regions were merged into the grassland region and the boreal, Canadian Shield, foothills, and Rocky Mountain regions were merged into the boreal region. This was done because the differentiation between water and land is distinctly different for forested areas versus low biomass grassland areas due to the lower backscatter of grasslands (Quegan et al. 2000; see Figures 2, 3, and 4).

Four ancillary datasets were used in the generation of the HTV layer or analysis of the results. Daily wind speed data from the NCEP Climate Forecast System Version 2 (Saha et al. 2014) was used to remove windy days. The SRTM 30 m DEM (USGS 2006) was used to derive slope for a slope mask while the Alberta Biodiversity Monitoring Institute (Alberta Biodiversity Monitoring Institute 2016) Human Footprint Inventory 2014 (HFI2014; ABMI Geospatial Centre 2017) was used for an agriculture and major roads mask. The Grasslands Vegetation Inventory

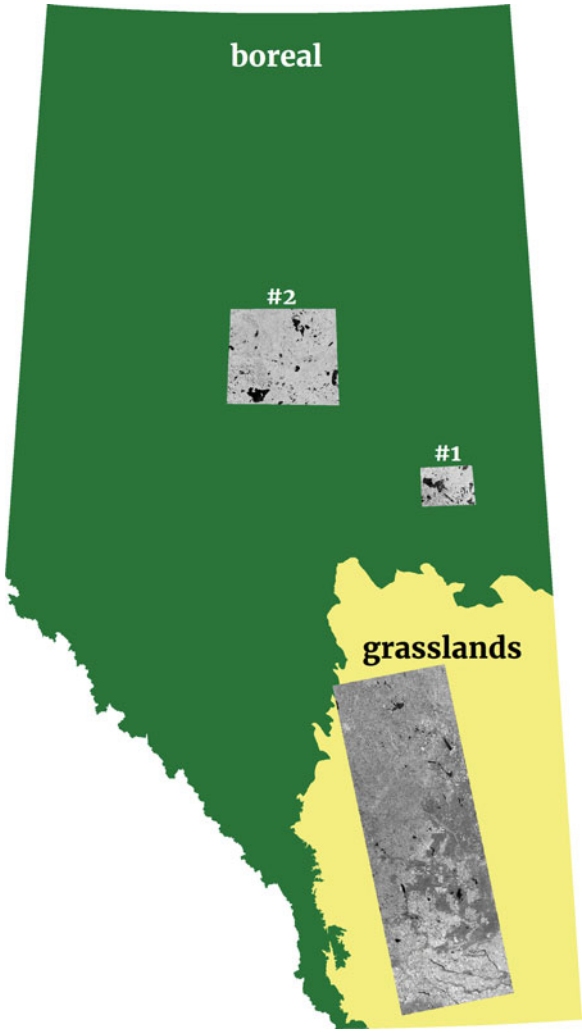

Figure 1. The spatial delineation of the boreal and grasslands processing regions with the three Sentinel-1 images used for thresholding decisions overlaid. The boreal and grasslands regions are delineated using the Natural Regions of Alberta.

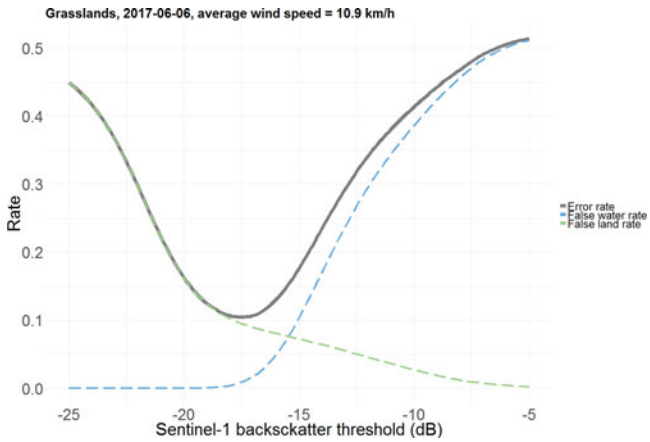

Figure 2. Errors rate of different Sentinel-1 backscatter thresholds for the grasslands test image. Image date from 2017-06-06 with an average wind speed of 10.9 km/h (from the Brooks Environment Canada weather station). The grey line represents the total error rate (false water + false land), the green line represents the false land rate, and the blue line represents the false water rate.

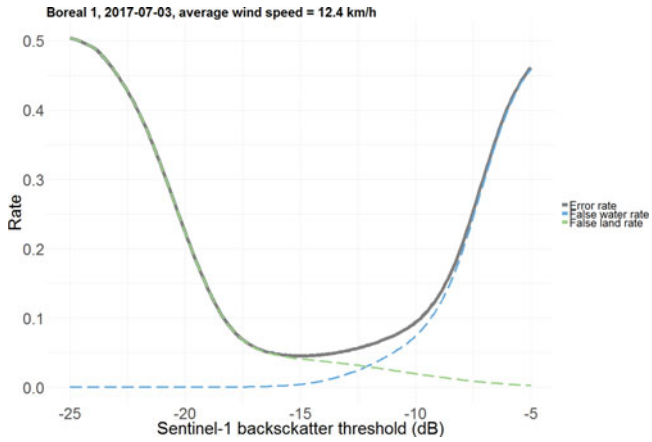

Figure 3. Errors rate of different Sentinel-1 backscatter thresholds for the boreal 1 test image. Image date from 2017-07-03 with an average wind speed of 12.4 km/h (from the Lac Le Biche Environment Canada weather station). The grey line represents the total error rate (false water + false land), the green line represents the false land rate, and the blue line represents the false water rate.

(Alberta Environment and Parks 2011), a polygon-based inventory describing land cover in the grasslands regions of Alberta, was used to mask out low biomass grasslands. Lastly, the Government of Alberta Base Features Hydrography Polygons (hereafter hydropoly; Alberta Environment and Parks, Government of Alberta 2004) was used as a training and analysis dataset.

Sentinel-1 thresholds

To generate the HTV layer, 2 important decisions needed to be made:

(*i*) Senintel-1 VV intensity threshold where a pixel is considered water; and

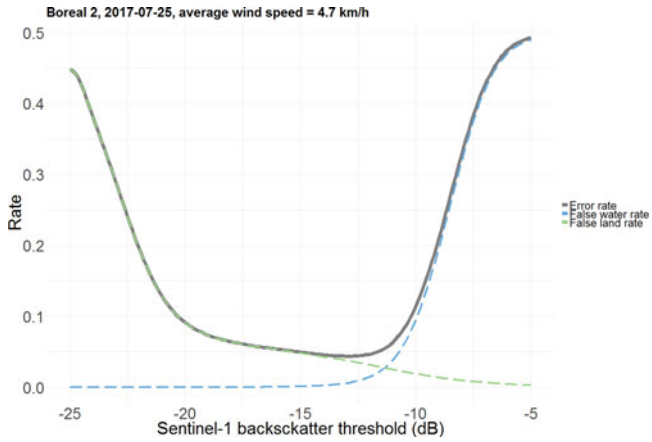

Figure 4. Errors rate of different Sentinel-1 backscatter thresholds for the boreal 2 test image. Image date from 2017-07-25 with an average wind speed of 4.7 km/h (from the Red Earth Creek Environment Canada weather station). The grey line represents the total error rate (false water + false land), the green line represents the false land rate, and the blue line represents the false water rate.

(*ii*) Wind speed threshold above which data should be removed from the HTV algorithm.

Three Sentinel-1 images from low wind speed days in 2017 (Figure 1) were analyzed to assess which Sentinel-1 backscatter threshold resulted in the lowest error rate for classifying water from land. Training water/land data was derived from the hydropoly layer. All permanent lakes were considered as water and land was considered any area without a hydropoly feature.

Figure 2 shows the error rate of different Sentinel-1 backscatter thresholds for differentiating water and land in the grasslands region. The lowest error rate (0.101) is seen at a threshold of –17.5 decibels (dB) with most of the error coming from false land errors. Figure 3 shows the error rate for a boreal image (boreal 1) with mixed forest and agriculture. The lowest error rate (0.049) is seen at a threshold of –15.1 dB with most of the error coming from false water pixels. Figure 4 shows the error rate for a boreal image (boreal 2) with continuous forest and minimal human footprint. A threshold of –13.7 dB generates the lowest error rate (0.048).

The data in Figure 2 show that an acceptable threshold for the grasslands region is –17.5 db. For this region it is expected that there will be an approximate error rate of 10% when classifying water and land. Figures 3 and 4 give different optimal thresholds for the boreal region (–15.1 and –13.7 dBs, respectively). Since false land error is preferred over false water error for this algorithm, the lower –15.1 dB threshold was chosen for the boreal region. Even with this lower threshold the boreal 2 image still has an error rate of only 5%. Therefore, in the boreal region we can expect an error rate of about 5% for classifying water.

Figure 5 shows the trend of increasing Sentinel-1 backscatter values with increased wind speed. A wind speed greater than 9 km/h was chosen as the threshold where data would be removed from the HTV algorithm. This was chosen since 90% of the data points in this threshold were below the –17.5 dB threshold. The authors acknowledge that this modeled wind data is too coarse to pick up on wind gusts or increase in speed over large lakes and, thus, we see a poor fit between the relation in wind speed and Sentinel-1 backscatter. However, the main goal of this threshold is to use "potentially" calm days but it is known that wind at the time of image acquisition may not have actually been calm.

HTV algorithm

To calculate HTV, each image was first turned into a binary "water" (1) and "non-water" (0) image. Any pixel below –17.5 and –15.1 dB for the grasslands and boreal zone, respectively, was considered water. To account for lake waves causing higher backscatter values, any pixel

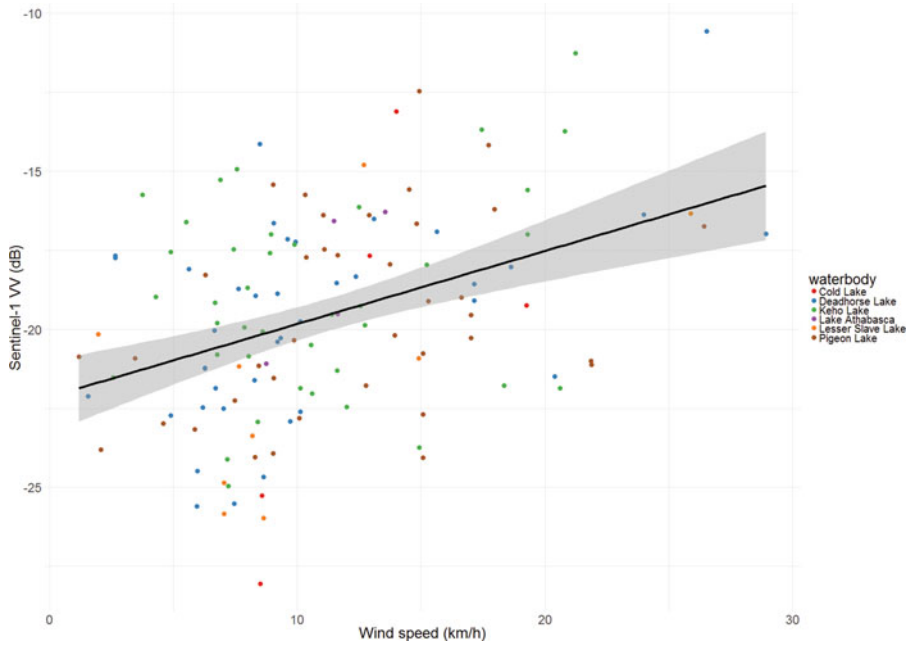

Figure 5. Wind speed (km/h) versus Sentinel-1 VV backscatter (dB) for six waterbodies across Alberta. With a fitted trend line ($R^2 = 0.15$).

where maximum wind speed, for the day of acquisition, above 9 km/h was removed (see Figure 5). To account for low backscatter values on the lee side of mountain slopes, all pixels with a slope value greater than 15 were removed from the analysis using SRTM DEM (USGS 2006). This was done based on visual interpretation of low backscatter values on parallel ridges corresponding to slopes over 15°. All pixels overlapping with cultivation or major roads (the ABMI Human Footprint Inventory for 2014 conditions; Alberta Biodiversity Monitoring Institute 2016) were assigned a value of zero. Finally, a grasslands mask was applied by masking out all grassland polygon habitat types from the Government of Alberta's Grassland Vegetation Inventory (Alberta Environment and Parks 2011). After all the thresholds and decisions, the binary water images were summed to get the number of times each pixel was classified as water. This was then divided by the number of pixels in the total pixel stack (after masking), multiplied by 100, and turned into integer format to get the percent of time a pixel was identified as water.

Comparison to Alberta Base Features Hydrography Polygons dataset

A comparison was done between the hydropoly layer and the HTV dataset. To see how the HTV data represented different waterbody types, permanent lakes, recurring lakes, and rivers were extracted from the hydropoly dataset. HTV values were extracted for each waterbody type and the distribution of values was plotted for each water body type. To test the effect of wind on lake size the area of permanent lakes was plotted against HTV value and a Generalized Additive Model curve was fitted to the data using R statistical software (R Core Team 2013). Finally, river width versus HTV value was investigated to determine the minimum river width, which can be detected by HTV data. Average river width was calculated by dividing the area of the river polygons by the length of the river lines. The mean HTV value was extracted for every river and compared to river width.

Results

In total, the HTV product created in the GEE environment used 125 billion pixels in the calculation (temporal pixel stack × number of 10-m pixels in Alberta). Figure 6 shows the pixel count used for calculations in the HTV dataset. This result shows a high of 65 for the southwest and 0 for a strip along Lake Athabasca.

The HTV layer is shown in Figure 7. This represents the percentage of time each pixel was identified as water. This layer maps the boundaries of waterbodies and gives an idea of how permanent they are and how much they fluctuate yearly or seasonally. Generally, land can be visualized with values of 0–10, recurring waterbodies with values of 11–65, and permanent lakes with values of 66–100. With this visualization it can be determined if each lake is permanent or recurring and it can also be used for delineating the permanent boundaries of lakes and the dynamic zones of lakes.

In a comparison to the hydropoly layer, the HTV layer was shown to have a higher value for permanent lakes with most permanent lakes having a HTV value ranging from 62–87 (Figure 8). Recurring lakes had a peak

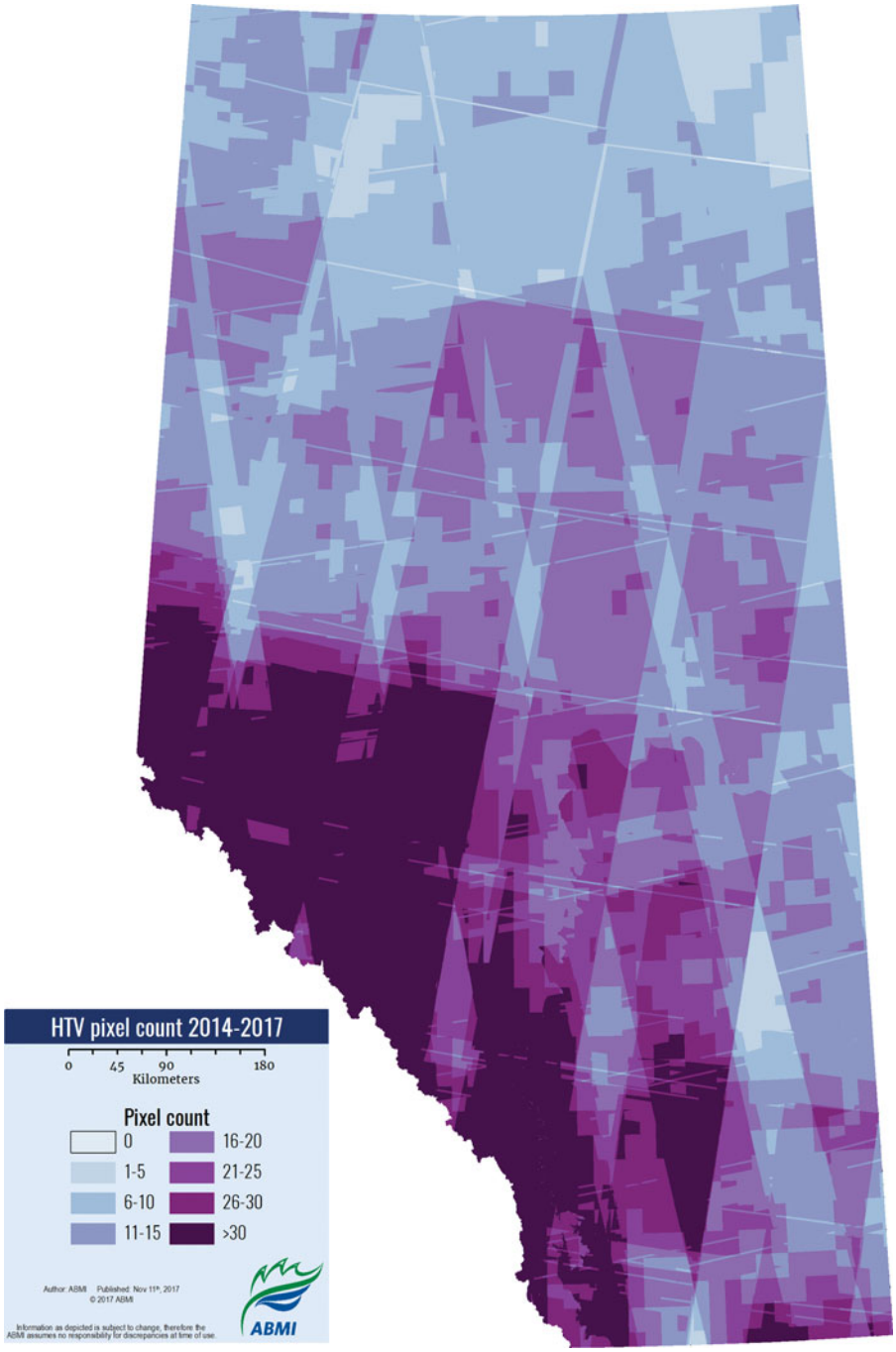

Figure 6. Pixel count of 10-m pixels used in the HTV calculation (wind speeds over 9 km/h removed).

distribution of HTV values at about 20 and very few with values over 60 (Figure 8). The majority of rivers had a low HTV value of 20–30 but there were some rivers with HTV values of 95–100, which was very rare in permanent and recurring lakes. Figure 9 shows an increasing trend in HTV values as lake size increases with a slight drop in HTV values for lake sizes of over 1,000 ha. Figure 10 shows a mean HTV value of near zero for any river with an average width of less than 30 m. Past an average width of 30 m, the mean HTV value increases sharply to a max of 80 at an average width of 1,000 m.

The problematic areas for this dataset are the low biomass grassland areas of southeast Alberta, the Rocky Mountains (southwest Alberta), and the sand dunes around Lake Athabasca (northeast Alberta). These areas have visible false water error but slope and grassland masking have helped minimize this error.

Discussion

Using the GEE platform allows streamlining and further advancement of this calculation intensive dataset across

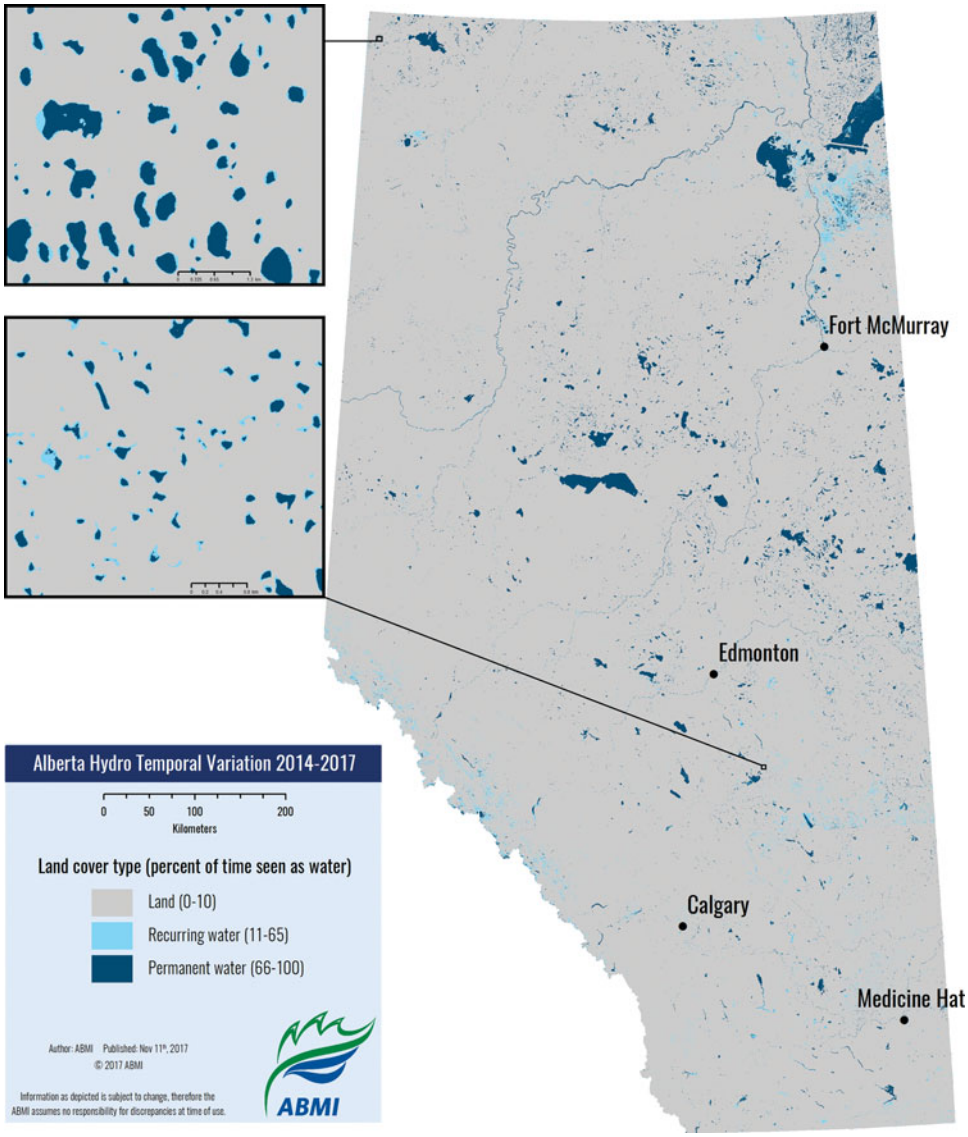

Figure 7. HTV for all of Alberta for the 2014 to 2017 time period. HTV values represented in three classes: land (HTV values 0–10)—where water is never or rarely seen; recurring water (11–65)—lakes which are seasonal or the area of lake level fluctuation around a permanent water body; and permanent water (66–100)—areas with consistent water. Inset areas provide more detail to show the dynamic regions around permanent lakes.

time and over large areas for any time period (post 2014). With adequate human footprint information, such as the ABMI Human Footprint Inventory, the dataset can be made more accurate since flat smooth human features can sometimes be seen as water with Sentinel-1 data.

The comparison to the hydropoly layer shows that the HTV dataset can differentiate permanent and recurring lakes (Figure 8). Many permanent lakes are in the HTV range of 62–87, which indicates that wind is still causing false land error. Some of the surprising results, such as low HTV values for permanent lakes, are expected since the training data used (hydropolys) is not up-to-date and the polygons do not match up well with the HTV data in some cases. The resolution of Sentinel-1 (Figure 10) also allows tracking larger rivers with a width greater than 30 m. Larger, windier permanent lakes may have an even larger issue with waves as lakes over 1,000 ha show a small decrease in the percent of time identified as water (Figure 9). Normally we would expect to see a steady increase in HTV values with size due to the edge effects of smaller waterbodies. A potential solution may be to use a permanent waterbody mask.

A problematic area still resides in the native grassland area of southeastern Alberta. The noise floor of Sentinel-1 makes it difficult to distinguish smooth or barren grasslands from water (Vachon and Wolfe 2008; Liu 2016). To solve this, grassland areas taken from a detailed grassland vegetation inventory were used to mask out these false water pixels. Another source of error was snow and ice. The chosen time range for the 2 zones was used to

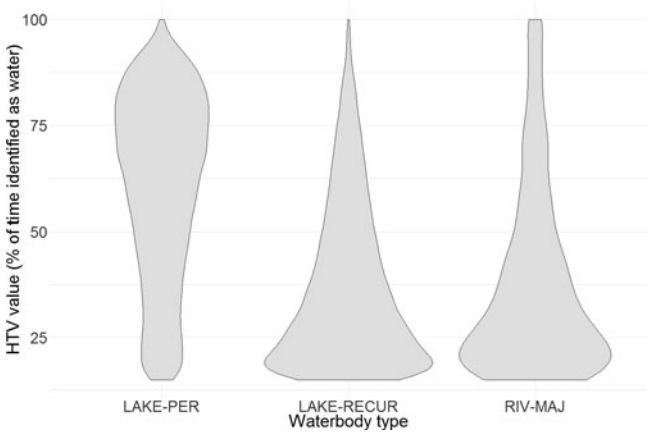

Figure 8. The HTV value distribution for three different waterbody types from the hydropoly layer. LAKE-PER = permanent lakes, LAKE-RECUR = recurring lakes, and RIV-MAJ = rivers. Lakes less than 1 ha were removed due to inaccurate mapping of the boundaries in many cases and lakes/rivers with HTV values below 15 were removed as these are likely lakes that no longer exist or recurring lakes that did not have water in them during the imaging time period. Note Lake Athabasca was eliminated from these statistics due to a pixel count of 0 in some areas of the lake.

minimize times where lakes were frozen. It appears this range works well except for the far north where visible ice breakup can be seen on the north side of Lake Athabasca (northeast Alberta). Snow, or more specifically, wet snow is also a source of error because the backscatter of wet snow and water is similar (Koskinen et al. 1997). This error is particularly evident in the Rocky Mountain region of Alberta. Mountain tops with low slope show HTV values of 30–50 indicating that there is wet snow or smooth ice there for 30%–50% of the time during May–September. This error may also occur more frequently in the northern areas of Alberta and it is acknowledged that

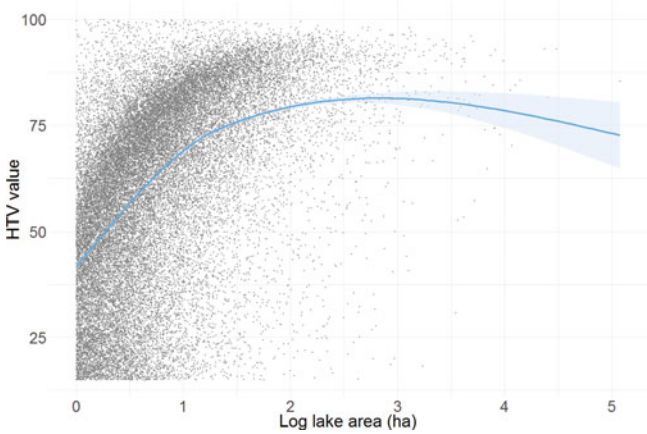

Figure 9. The HTV value of permanent lakes versus the log of the lake area in hectares. Fitted curve (blue) with error bounds is generated with gam method in R Statistical Software (R Core Team, 2013). Lakes with HTV values of below 15 were removed. Note Lake Athabasca was eliminated from these statistics due to a pixel count of 0 in some areas of the lake.

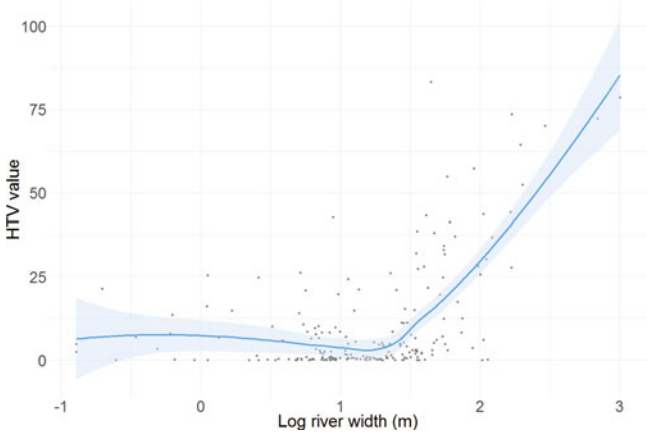

Figure 10. The mean HTV value of rivers from the Government of Alberta hydropoly layer versus the log of river width in meters. Fitted blue curve (blue) with error bounds is generated with loess method in R Statistical Software (R Core Team, 2013).

the inability to distinguish wet snow from water is a limitation of the dataset. Overall, the mean error of each individual image water/land classification is expected to be about 10% with more error occurring in the grassland and mountain regions (Figures 2–4). It is expected that heavily forested areas with limited human development will have very low error rates of around 5% (Figures 3 and 4).

The biggest improvement that could be made to the current dataset would be a new data source for wind speed. The current wind speed data is based off a model and has a 12 km × 20 km cell size. This means the data is too coarse to pick up on local variation in wind and does not necessarily reflect the wind seen at the time of image acquisition. Figure 5 shows that an increase in wind speed from the NCEP Climate Forecast System does cause an increase in Sentinel-1 backscatter but the relationship is not strong, likely due to the reasons described above. Therefore, the wind filter does not remove windy condition data but rather it removes days that have the potential for high wind. The main reason for using this data is its integration in the GEE environment, which allows for the seamless integration of weather data with remote sensing data. Weather station data could be used in the algorithm but this would require the generation of 640 daily wind speed grids and the loading into the GEE environment. Weather station data also presents the issue of sparse station data in northern Alberta. This algorithm should intend to use the best weather data available for the given area. For example, the algorithm used anywhere in the United States should use the Real-time Mesoscale Analysis Products, which give hourly weather analysis at a 2-km scale (National Centers for Environmental Prediction 2013).

Overall this study provides a methodological framework for building a surface water variation dataset within

the GEE environment. Backscatter thresholds will vary from region to region and more work on optimal water classification thresholds will be valuable for improving the accuracy of these datasets. Further exploration into the proper use of wind speed data and new wind speed data will be vital to improving the results. Incorporating wind direction with respect to sensor look direction (Ulaby et al. 1986) may also be a potential advancement for the HTV algorithm.

Conclusions and outlook

The results of the HTV layer demonstrate great potential for monitoring the annual and inter-annual variation of surface water extent in Alberta. Overall, this dataset provides an example of a robust methodology for developing a hydro temporal variation dataset. The 2014–2017 time period may be limited in some areas due to a lower number of available images, i.e., lower pixel count. This methodology is promising for 2018 data and future years as the Sentinel-1 archive continues to grow. Eventually, this process could lead to dynamic surface water maps with weekly-biweekly updates. This near real time dataset could then be summarized into the HTV dataset yearly to get a similar product to the 1 described in this article. Theoretically, this methodology could be adjusted and applied globally, although mountainous areas and barren low biomass ecosystems will need further testing and assessment, as they may produce more spurious results than native vegetation, higher biomass ecosystems. This method could possibly be advanced with the RADARSAT Constellation Mission (RCM; Canadian Space Agency 2017) due to the higher temporal resolution, greater availability of HH and HV polarizations, and lower noise floor compared to Sentinel-1. The combination of freely available Sentinel-1 SAR, future RCM data, and GEE's processing power provides an exciting future for weekly, seasonal, and yearly dynamic surface water maps.

References

Alberta Biodiversity Monitoring Institute Geospatial Centre. 2017. *Human Footprint Inventory 2014—Public Version, Version 2*. Edmonton, Alberta, Canada: Alberta Biodiversity Monitoring Institute Geospatial Centre.

Alberta Biodiversity Monitoring Institute. 2016. *ABMI Photo-Plot Quality Control Manual*. Edmonton, Alberta.

Alberta Environment and Parks, Government of Alberta. 2004. *Base Water Polygon*. Edmonton, Alberta, Canada: Alberta Environment and Parks, Government of Alberta.

Alberta Environment and Parks. 2011. *Grassland Vegetation Inventory (GVI) Specifications*. Edmonton, Alberta, Canada.

Alberta Parks. 2015. *Natural Regions and Subregions of Alberta: A Framework for Alberta's Parks*. Edmonton, Alberta: Alberta Tourism, Parks and Recreation.

Bartsch, A., Wagner, W., Scipal, K., Pathe, C., Sabel, D., and Wolski, P. 2009. "Global monitoring of wetlands—The value of ENVISAT ASAR global mode." *Journal of Environmental Management*, Vol. 90: pp. 2226–2233.

Bolanos, S., Stiff, D., Brisco, B., and Pietroniro, A. 2016. "Operational surface water detection and monitoring using Radarsat 2." *Remote Sensing*, Vol. 8(No. 4): pp. 285.

Brisco, B. 2015. "Mapping and monitoring surface water and wetlands with synthetic aperture radar." In: *Remote Sensing of Wetlands: Applications and Advances*. edited by R.W. Tiner, M.W. Lang, and V.V. Klemas, pp. 119–136. Boca Raton, FL: CRC Press.

Brisco, B., Short, N., van der Sanden, J.J., Landry, R., and Raymond, D. 2009. "A semi-automated tool for surface water mapping with RADARSAT-1." *Canadian Journal of Remote Sensing*, Vol. 35: pp. 336–344.

Brisco, B., Touzi, R., van der Sanden, J.J., Charbonneau, F., Pultz, T.J., and D'Iorio, M. 2008. "Water resource applications with RADARSAT-2—A preview." *International Journal of Digital Earth*, Vol. 1(No. 1): pp. 130–147.

Canadian Space Agency. 2017. "RADARSAT constellation." www.asc-csa.gc.ca/eng/satellites/radarsat/. Accessed May 15, 2017.

European Space Agency. 2014, 2015, 2016. "Copernicus Sentinel-1 data."

Ding, X.W., and Li, X.F. 2011. "Monitoring of the water-area variation of Lake Dongting in China with ENVISAT ASAR images." *International Journal of Applied Earth Observation and Geoformation*, Vol. 13(No. 6): pp. 894–901.

Ducks Unlimited. 2017. "Wetlands." www.ducks.ca. Accessed May 2, 2017.

Environment and Climate Change Canada. 2015. *The National Hydrological Service*. Ottawa, Ontario, Canada: Environment and Climate Change Canada.

Gauthier, Y., Bernier, M., and Fortin, J.-P. 1998. "Aspect and incidence angle sensitivity in ERS-1 SAR data." *International Journal of Remote Sensing*, Vol. 19(No. 10): pp. 2001–2006.

Google Earth Engine Team. 2015. "Google Earth Engine: A planetary-scale geospatial analysis platform." https://eathengine.google.com. Accessed May 6th, 2017.

Gstaiger, V., Huth, J., Gebhardt, S., Wehrmann, T., and Kuenzer, C. 2012. "Multi-sensoral and automated derivation of inundated areas using TerraSAR-X and ENVISAT ASAR data." *International Journal of Remote Sensing*, Vol. 33(No. 22): pp. 7291–7304.

Henderson, F., and Lewis, A. 1998. *Manual of Remote Sensing: Principles and Applications of Imaging Radar*. New York, NY: Wiley.

Hoerling, M., and Kumar, A. 2003. "The perfect ocean for drought." *Science*, Vol. 299(No. 5607): pp. 691–694.

Kasischke, E.S., and Bourgeau-Chavex, L.L. 1997. "Monitoring south Florida wetlands using ERS-1 SAR imagery." *Photogrammetry Engineering and Remote Sensing*, Vol. 63 (No. 3): pp. 281–291.

Koskinen, J.T., Pulliainen, J.T., and Hallikainen, M.T. 1997. "The use of ERS-1 SAR data in snow melt monitoring." *IEEE Transaction on Geoscience and Remote Sensing*, Vol. 35 (No. 3): pp. 601–610.

Lee, J.-S., Wen, J.-H., Ainsworth, T.L., Chen, K.-S., and Chen, A.J. 2009. "Improved sigma filter for speckle filtering of SAR imagery." *IEEE Transactions on Geosciences and Remote Sensing*, Vol. 47(No. 1): pp. 202–213.

Li, J., and Wang, S. 2015. "An automated method for mapping inland surface waterbodies with Radarsat-2 imagery." *International Journal of Remote Sensing*, Vol. 36: pp. 1367–1384.

Liu, C. 2016. "Analysis of Sentinel-1 SAR data for mapping standing water in the Twente region." Masters Thesis, University of Twente.

Malenovsky, Z., Rott, H., Chihar, J., Schaepman, M.E., Garcia-Santos, G., Fernandes, R., and Berger, M. 2012. "Sentinels for science: Potential of Sentinel-1, -2, and -3 missions for scientific observations of ocean, cryosphere, and land." *Remote Sensing of Environment*, Vol. 120: pp. 91–101.

Martinis, S., Twele, A., and Voigt, S. 2009. "Towards operational near real-time flood detection using a split-based automatic thresholding procedure on high resolution TerraSAR-X data." *Natural Hazards Earth System Science*, Vol. 9: pp. 303–314.

National Centers for Environmental Prediction. 2013. *Real-Time Mesoscale Analysis Products*. College Park, MD: University of Maryland.

Pekel, J.-F., Cottam, A., Gorelick, N., and Delward, A.S. 2016. "High-resolution mapping of global surface water and its long term changes." *Nature*, Vol. 540: pp. 418–422.

Pultz, T.J., Crevier, Y., Brown, R.J., and Boisvert, J. 1997. "Monitoring of local environmental conditions with SIR-C/X-SAR." *Remote Sensing of Environment*, Vol. 59(No. 4): pp. 248–255.

Quegan, S., Le Toan, T., Yu, J.J., Ribbes, F., and Floury, N. 2000. "Multitemporal ERS SAR analysis applied to forest mapping." *IEEE Transactions of Geoscience and Remote Sensing*, Vol. 38(No. 2): pp. 741–753.

R Core Team. 2013. "R: A language and environment for statistical computing. R Foundation for Statistical Computing." Vienna, Austria. http://www.R-project.org/. Accessed April 20, 2017.

Saha, S., Moorthi, S., Wu, X., Wang, J., Nagdiga, S., Tripp, P., Behringer, D., et al. 2014. "The NCEP climate forecast system Version 2." *Journal of Climate*, Vol. 27: pp. 2185–2208.

Santoro, M., and Wugmüller, U. 2014. "Multi-temporal synthetic aperture radar metrics applied to map open water bodies." *IEEE Journal of Selected Topics in Applied Earth Observations and Remote Sensing*, Vol. 7(No. 8): pp. 3225–3238.

Santoro, M., Wugmüller, U., Lamarche, C., Bontemps, S., Defourny, P., and Arino, O. 2015. "Strengths and weaknesses of multi-year Envisat ASAR backscatter measures to map permanent open water bodies at global scale." *Remote Sensing of Environment*, Vol. 171: pp. 185–201.

Schindler, D.W., and Donahue, W.F. 2006. "An impending water crisis in Canada's western prairie provinces." *PNAS*, Vol. 103(No. 19): pp. 7210–7216.

Townsend, P.A. 2002. "Relationship between forest structure and the detection of flood inundation in forested wetlands using C-band SAR." *International Journal of Remote Sensing*, Vol. 23: pp. 443–460.

Töyrä, J., and Pietroniro, A. 2005. "Towards operational monitoring of a northern wetland using geomatics-based techniques." *Remote Sensing of Environment*, Vol. 97(No. 2): pp. 174–191.

Töyrä, J., Pietroniro, A., and Martz, L.W. 2001. "Multi sensor assessment of freshwater wetland." *Remote Sensing of Environment*, Vol. 75(No. 2): pp. 162–173.

Twele, A., Cao, W., Plank, S., and Martinis, S. 2016. "Sentinel-1-based flood mapping: A fully automated processing chain." *International Journal of Remote Sensing*, Vol. 37(No. 13): pp. 2990–3004.

Ulaby, F.T., Moore, R.K., and Fung, A.K. 1986. *Microwave Remote Sensing: Active and Passive. Volume III: From Theory to Applications*. Norwood, MA: Artech House.

USGS. 2006. *Shuttle radar topography mission*. College Park, Maryland: Global Land Cover Facility, University of Maryland.

Vachon, P.W., and Wolfe, J. 2008. *Validation of ship signatures in Envisat ASAP AP mode data using AISLive*. Ottawa, Ontario: Defence R&D.

White, L., Brisco, B., Pregitzer, M., Tedford, B., and Boychuk, L. 2014. "RADARSAT-2 beam mode selection for surface water and flooded vegetation mapping." *Canadian Journal of Remote Sensing*, Vol. 40: pp. 135–151.

Wilson, A.M., and Jetz, W. 2016. "Remotely sensed high-resolution cloud dynamics for predicting ecosystem and biodiversity distributions." *PLoS Biology*, Vol. 14(No. 3): pp. 1–20.

Yesou, H., Huber, C., Haouet, S.L., X., Huang, S., Frainpoint, P.D., and Desnos, Y.L. 2016. "Exploiting Sentinel 1 time series to monitor the largest fresh water bodies in PR China, the Poyang Lake." Paper presented at the 2016 IEEE Geoscience and Remote Sensing Symposium (IGARSS), Beijing, China, July 2016.